

# Retardation magnification and the appearance of relativistic jets<sup>\*</sup>

Sebastian Jester<sup>†‡</sup>

*Max-Planck-Institut für Astronomie, Königstuhl 17, 69117 Heidelberg, Germany*

13 June 2021

## ABSTRACT

Thanks to the availability of high-resolution high-sensitivity telescopes such as the Very Large Array, the *Hubble Space Telescope*, and the *Chandra X-ray Observatory*, there is now a wealth of observational data on relativistic jets from active galactic nuclei (AGN) as well as galactic sources such as Black-Hole X-ray Binaries. Since the jet speeds cannot be constrained well from observations, but are generally believed to be relativistic, physical quantities inferred from observables are commonly expressed in terms of the unknown beaming parameters: the bulk Lorentz factor and the line-of-sight angle, usually in their combination as relativistic Doppler factor. This paper aims to resolve the discrepancies existing in the literature about such “de-beaming” of derived quantities, in particular regarding the minimum-energy magnetic field estimate. The discrepancies arise because the distinction is not normally made between the case of a fixed source observed with different beaming parameters and the case where the source projection on the sky is held fixed. The former is usually considered, but it is the latter that corresponds to interpreting actual jet observations. Furthermore, attention is drawn to the fact that apparent superluminal motion has a spatial corollary, here called “retardation magnification”, which implies that most parts of a relativistic jet that are actually present in the observer’s frame (a “world map” in relativity terminology) are in fact hidden on the observer’s image (the “world picture” in general, or “supersnapshot” in the special case of astronomy).

**Key words:** Galaxies: jets – ISM: jets and outflows – Relativity

## 1 INTRODUCTION

For over 50 years from the appearance of the seminal *Zur Elektrodynamik bewegter Körper* (Einstein 1905), only the Lorentz transformations of the 4-coordinates of “events” were considered in the literature, but not how relativistically moving bodies would *appear* when looked at or photographed. This was first done independently and (relatively) simultaneously by Penrose (1959) and Terrell (1959); the former showed that the projected outline of a relativistically moving sphere is always a circle, while the latter provided a more extensive discussion of the appearance of moving bodies and pointed out the key features of observing relativistically moving bodies: they appear both *rotated* and *scaled* (more details will be given below).

The motivation for writing the present paper is work on interpreting observations of relativistic jets (Jester et al. 2006, e.g.), where the need arises to infer physical properties of the jet fluid

in its own rest frame from observations, subject to corrections due to relativistic beaming, whose magnitude is, however, not known from observations. A particular quantity of interest is the rest-frame minimum-energy magnetic-field estimate for a synchrotron source (Burbidge 1959), and there are different opinions in the literature about how the true rest-frame minimum-energy field scales with the relativistic Doppler factor compared to that inferred assuming a non-relativistic source (compare eqn. A3 of Stawarz et al. 2003 to eqn. A7 of Harris & Krawczynski 2002). Some of the argument revolves around whether the observed morphological features of jets are “blobs” or “jets”, and their (apparently) different beaming properties.

Given these differences of opinion on how to “de-beam” properly, it is perhaps surprising that NASA’s Astrophysics Data System lists only three papers on interpreting jet observations as citing Terrell (1959), and his results do not seem to be part of the common knowledge of jet researchers. One of the citing papers is Lind & Blandford (1985), who consider the implications of relativistic beaming on the difference between observed and intrinsic source counts and give detailed formulae for relating observed and jet-frame fluxes and emissivities. Some of these formulae had already been presented in the seminal paper by Blandford & Königl (1979).

It appears that the difficulties in interpreting jet observations arise because the problem under consideration is ill-posed. As will

<sup>\*</sup> Accepted by MNRAS 2008 June 23. Received 2008 June 23; in original form 2008 February 23.

<sup>†</sup> Portions of this work were carried at the Particle Astrophysics Center, Fermilab MS 127, PO Box 500, Batavia, IL 60510, USA; and while the author was an Otto Hahn fellow of the Max-Planck-Gesellschaft at the Department of Physics and Astronomy, University of Southampton, Southampton SO17 1BJ, United Kingdom

<sup>‡</sup> E-mail: jester@mpia.de

be argued in detail below, what matters for interpreting jet observations subject to unknown beaming parameters is that we have observed the 2-dimensional projection of a source’s appearance onto the plane of the sky and try to infer the source’s rest-frame properties from this projection. Confusion arises because most formulae in the literature consider what happens to the observed quantities when a *fixed source* moves with different Lorentz factors and at different line-of-sight angles to the observer, while in observations, it is the *projection* of the source which is held constant. Furthermore, the effects of light-travel time delays along the line of sight are typically only mentioned explicitly in work comparing jet simulations to observations, e.g., in Aloy et al. (2003) and Swift & Hughes (2008), but not in the observational literature. This and the preference for adopting the fixed-source view may be related to the fact that Lorentz transformations are usually covered in great detail in a typical course on special relativity, but Penrose (1959) and Terrell (1959) are hardly mentioned in relativity textbooks.

This leads to the present paper with the following outline: the remainder of the introduction summarizes the results by Penrose (1959) and Terrell (1959) and sets out some basic definitions and terminology. The appearance of relativistic objects, and in particular of astrophysical jets, is discussed in §2, both from a theoretical point of view and using a simple ray-tracer. Ready-to-use formulae for relating jet-frame quantities to observables are given in §3, including the minimum-energy field. The discussion and summary are given in §4, while Appendix A describes some *Gedankenexperimente* on non-conventional world-map measurements that lead to length expansion and time acceleration.

### 1.1 World Pictures and Supersnapshots

As first noted by Terrell (1959), there is a fundamental difference in relativity between the *locations* (4-coordinates) of events as judged by observers that are local to the events and equipped with sets of clocks that are synchronized in their rest frame, and the *appearance* of relativistically moving bodies as judged by distant observers by means of photons that are received simultaneously; a little earlier, Penrose (1959) had considered the special case of the observed outline of a relativistically moving sphere. The set of event locations is a *world map*, while the picture that is taken of the events is a *world picture*. In the special case of photons arriving at right angles to the detector taking the world picture, it is called a *supersnapshot* (Rindler 1977). Astronomical observations clearly fall under the definition of a supersnapshot.

The appearance of relativistically moving objects in a supersnapshot is governed by two aspects of photon paths in special relativity (Terrell 1959; Rindler 1977; Lind & Blandford 1985):

(i) Two photons traveling abreast with a separation  $\Delta s$  in one frame (i.e., photons traveling “alongside each other” with  $\Delta s$  measured perpendicular to their direction of motion) do so in *all* frames. This is the case because  $|\Delta s|^2$  is invariant under Lorentz transformations and  $\Delta s$  is a space-like interval.

(ii) If a photon is traveling at an angle  $\theta'$  to the direction of motion of some frame that is moving with speed  $\beta c$  and Lorentz factor  $\Gamma = (1 - \beta^2)^{-1/2}$  with respect to an observer, the angle between the direction of motion and the photon direction in that frame is related to the angle  $\theta$  between the direction of motion and the photon direction in the observer’s frame by

$$\mu' = \frac{\mu - \beta}{1 - \beta\mu}, \quad (1)$$

where  $\mu = \cos \theta$  etc., or, equivalently,

$$\sin \theta' = \delta \sin \theta, \quad (2)$$

where  $\delta$  is the relativistic Doppler factor

$$\delta = [\Gamma(1 - \beta\mu)]^{-1}. \quad (3)$$

The latter phenomenon is the well-known angle aberration; the former is perhaps less well-known, but essential for the analysis of images of relativistically moving objects, and implies that the supersnapshot is a *scaled* version of the rest-frame image. Taken together, they yield Terrell’s result that the appearance of such an object in a supersnapshot is simply the object’s appearance as seen from the aberrated angle  $\theta'$  in its rest frame, with its apparent size along the direction of motion scaled by the Doppler factor  $\delta$ .

As a consequence of eq. (1), even approaching objects appear to be seen “from behind” unless  $\mu < \beta$ , i.e.,  $\delta > \Gamma$ ; in the limiting case  $\mu = \beta \Leftrightarrow \delta = \Gamma \Leftrightarrow \sin \theta = 1/\Gamma$ , a relativistic object is seen exactly side-on in its rest frame and with exactly its rest-frame length as its “projected” length.

### 1.2 Terminology: “Blobs” versus “jets” versus “shocks” – at rest in different frames

It is useful clearly to set out the terminology for the remainder of the paper, because the brightness pattern observed in astrophysical jets can be at rest in frames that are different from both the observer frame, and the fluid rest frame, as discussed in detail by Lind & Blandford (1985). Their discussion and notation is adopted here. It distinguishes between “blob”, “jet” and “shock” features, which are defined by being at rest in one of three frames relevant to the problem. Thus, it is useful to give the definitions of the relevant frames together with those of the morphological terms:

(i) The “observer frame” is that in which the astronomer is at rest. Once appropriate cosmological corrections are applied, the observer frame is conceptually identical to the frame in which the jet source and its host are at rest.

A “jet” feature is then a *resolved* brightness pattern whose outline is at rest in the observer frame. Observer-frame quantities have no primes, e.g.  $j$  for volume emissivity.

(ii) The “fluid frame” is the rest frame of the emitting fluid, which is taken to be moving through the observer frame at relativistic speed. The term “rest frame” is used interchangeably with “fluid frame”.<sup>1</sup>

A “blob” or “plasmoid” is a brightness pattern whose outline is at rest in the fluid frame. Fluid-frame quantities will be designated by double primes, e.g.  $j''$ .

(iii) A “pattern” or “shock” feature is a brightness pattern whose outline is at rest neither in the fluid nor in the observer frame, e.g., a shock traveling through the jet fluid. It defines the third frame, the frame in which this pattern is at rest. Pattern-frame quantities have single primes, e.g.  $j'$ . The emissivity of the fluid traveling through such a “shock” transforms according to the fluid’s Doppler factor  $\delta''$ , while its projected appearance and morphology are governed by the shock’s Doppler factor  $\delta'$ .

<sup>1</sup> The emitting fluid is not necessarily identical with that carrying the bulk of the jet’s kinetic energy, nor are those two fluids necessarily moving at the same speed (Harris & Krawczynski 2007). However, this distinction does not affect the relation between observables and physical quantities in the rest frame of the emitting fluid, which is the subject of this paper. Nevertheless, it needs to be kept in mind when interpreting fluid-frame quantities.

These are fairly intuitive definitions. Nevertheless, the difference between the “blob” and “jet” formulae in eqn. C7 of Begelman et al. (1984) is just one of *choice of integration boundaries*, and in particular whether the integration boundaries are held fixed in the observer frame when  $\delta$  is changed (jet case) or are allowed to vary according to the different projected morphology of a “blob” under changes of  $\delta$ . Thus, it is possible to apply a “jet” formula to a small segment of a blob as long as the integration boundaries are held fixed in the observer frame. In §§3.1.3 and 3.2.3 below, I will present detailed formulae for converting observed to fluid-frame properties in each case, with expressions for the minimum-energy field in §3.3.2.

### 1.3 Basic definitions and beaming formulae

This section summarizes the basic definitions of surface brightness/intensity, flux density and luminosity of astronomical sources, as well as the beaming properties of blobs, jets, and shocks. I will give explicit formulae for observed surface brightness and total flux in terms of source parameters for simple geometries, as well as ray-tracing images showing the appearance of such sources in supersnapshots.

For the computation of surface brightness and flux, I use the notation and formulae as given by Blandford & Königl (1979) and Lind & Blandford (1985), assuming an optically thin, isotropic emission with a power-law emissivity  $j_\nu \propto \nu^\alpha$  that is constant within the emitting region. All observables will be expressed in terms of the emissivity  $j''$  in the fluid rest frame and the source size in the pattern frame  $\Sigma'$ , which is identical to the fluid and observer frame for a “blob” and “jet”, respectively. Cosmological transformations, however, are not always given explicitly in order to simplify the notation; they can be re-incorporated in the usual way by inserting appropriate powers of  $(1+z)$  for cosmological redshifts, and using the appropriate cosmological distance measures.

The surface brightness or intensity  $I$ , flux density  $S_\nu$  and luminosity  $L$  of a source are given by

$$I_\nu = \int_0^s j_\nu dx, \quad (4)$$

$$S_\nu = \int_A I_\nu dA \quad (5)$$

$$= d_L^{-2} \int_V j_\nu dV, \quad (6)$$

$$L_\nu = 4\pi d_L^2 S_\nu \quad (7)$$

$$= 4\pi \int_V j_\nu dV,$$

where  $d_L$  is the luminosity distance to the source, which has specific emissivity  $j$ , volume  $V$  and projected surface area  $A$ .

The transformation properties of these quantities then follow from the relativistic invariance of  $I_\nu/\nu^3$  and the volume transformation (taken from Appendix C of Begelman et al. 1984):

$$\nu = \delta'' \nu'' \quad (8)$$

$$d\Omega = \delta''^{-2} d\Omega'' \quad (9)$$

$$I_\nu(\nu) = \delta''^3 I''_{\nu''}(\nu'') \quad (10)$$

$$j_\nu(\nu) = \delta''^2 j''_{\nu''}(\nu'') \quad (11)$$

Assuming optically thin emission makes the discussion appropriate for arcsecond-scale jets, where sources are not compact enough for self-absorption to become important. The difficulties of in-

terpreting observations of optically thick sources, such as compact cores and milli-arcsecond scale jets, have been highlighted by Blandford & Königl (1979) and Lind & Blandford (1985). The essential point here is that the appearance of optically thick sources varies as function of viewing direction, and the relativistic angle aberration implies that the beamed appearance is governed by this intrinsic viewing angle dependence in addition to the flux and surface brightness beaming. The volume transformation deserves separate consideration.

### 1.4 Volume transformation of relativistic objects in astronomical images

The fact that the outline of the different kinds of brightness pattern is at rest in different frames has led some authors to write down different volume transformation formulae for astronomical observations of “jets” and “blobs” (see Sikora et al. 1997, Appendix A, and Stawarz et al. 2003, Appendix A, e.g.). However, what matters for the volume transformation of a feature identified in an astronomical image or radio map is only that the image is a supersnapshot. What matters for the interpretation of the supersnapshot is the volume of fluid whose photons arrive simultaneously on the *supersnapshot*, not the volume of fluid that is located within the jet volume in the *world map*. Hence, the correct volume transformation for any fluid volume  $V''$  observed by means of a supersnapshot is

$$V = \delta'' V'', \quad (12)$$

where  $\delta''$  is the Doppler factor of the fluid in the observer frame.

If the decisive criterion was not the fact that astronomical observations are supersnapshots, one could argue with equal justification that the correct volume transformation formula for the fluid in a jet section is  $V'' = V/\Gamma$  because the jet volume is at rest in the observer frame and hence appears contracted in the rest frame of the fluid, or alternatively that the correct transformation is  $V'' = V \times \Gamma$  because the fluid is moving through the observer frame, and therefore *it* is contracted. Both can of course be correct, depending on whether one is judging the jet volume with the help of events that are simultaneous in the fluid or the observer frame. However, a supersnapshot corresponds to neither world-map case — the supersnapshot criterion is photons *arriving* simultaneously at the observer, which nearly always does not correspond to photons *being emitted* simultaneously in any frame.

That eq. (12) is correct for both the “jet” and “blob” case can be seen also by considering a section of a “jet” as a collection of infinitesimal blobs that are each at rest in the fluid frame. Alternatively, a “jet” can be considered as a section of a “blob” that is moving through a transparent gap in obscuring material that is at rest in the observer frame — if 90% of a blob’s volume is covered in the observer frame, the rest-frame volume of the visible part is 10% of the blob’s total observer-frame volume, and hence must also be 10% of the blob’s rest-frame volume.

As an alternative derivation of eq. (12), consider that the observer-frame volume of a “jet” or “blob” (or an infinitesimal element of it) is given by

$$V = s \times l \times h,$$

where  $s$  is its extent transverse to the line of sight in the plane of its motion,  $h$  is the extent perpendicular to both the line of sight and the direction of motion, and  $l$  is along the line of sight. The individual factors of  $V$  transform into the fluid rest frame as follows.

First, since  $h$  is perpendicular to the direction of motion, it is not affected by relativity in any way, and  $h'' = h$ . Next, recall

from §1.1 above that the transverse separation  $\Delta s$  of two photon paths, i.e., light rays, is Lorentz-invariant. The transverse extent  $s$  is defined by two such parallel light rays and therefore it is also Lorentz-invariant, hence  $s'' = s$ . Finally, to determine the transformation properties of  $l$ , consider the following argument. The optical depth  $\tau$  along  $l$  has to be Lorentz-invariant since it encodes the fraction  $e^{-\tau}$  of photons that are absorbed by the jet material, which is independent of the motion of any observer (Rybicki & Lightman 1979, p. 147). By definition, the optical depth is

$$\tau = l \kappa_\nu,$$

where  $\kappa_\nu$  the absorption coefficient of the material. The Lorentz invariance of  $\tau$  therefore implies that  $l$  transforms inversely to  $\kappa_\nu$ . From the Lorentz invariance of  $\nu \kappa_\nu$  (again see Rybicki & Lightman 1979), it follows that  $l$  transforms as  $\nu$ , i.e.,  $l = \delta'' l''$ . Hence  $V = s l h = s \delta'' l'' h = \delta'' s'' l'' h'' = \delta'' V''$ , again yielding eq. (12).

Thus, the relation between rest-frame and observer-frame volume for supersnapshots is always given by eq. (12), no matter whether we are considering a “jet”, “blob” or even “shock” feature. As noted at the end of the preceding section, the well-known apparent difference between the beaming formulae for a blob and a jet ( $\delta^{2-\alpha}$  versus  $\delta^3$ , such as in App. C7 of Begelman et al. 1984) is in fact just a difference of *integrands*; since the *integration boundaries* differ depending on whether an object is considered as blob or jet, the final answer is independent of the assumed geometry. In other words, **jets and blobs have the same beaming properties if identical source volumes are considered**. The equivalence of jet and blob formulae will be shown explicitly in §3.2.3 and 3.3.2 below.

While eq. (12) appears straightforward to interpret, the supersnapshot is merely a projection of the observer-frame volume onto the plane of the sky, so that **the observer-frame volume  $V$  is not a direct observable** (see Fig. 4 below). Therefore, the volume formula can only be used for interpreting astronomical images if an assumption is made about the geometry of the source. However, its use in determining observables from known rest-frame quantities is straightforward.

## 2 THE APPEARANCE OF RELATIVISTIC OBJECTS

This section attempts to give an intuitive pictorial representation of how relativistic jets appear in supersnapshots. The first part considers jet observations as supersnapshots of infinitesimally thin relativistic rods. This approach is appropriate for demonstrating how the scale change in a supersnapshot, referred to below as *retardation magnification*, arises as spatial corollary to the well-known temporal phenomenon of apparent superluminal motion (Rees 1966). The second part presents results from a ray-tracer that demonstrate the differences between world maps and world pictures. Those effects are particularly important which arise from the extent of actual jets perpendicular to the direction of motion, as they results in extra light-travel delays between the near and far side of the jet that are not present in the case of an idealized, thin rod.

### 2.1 Retardation magnification and hiding

#### 2.1.1 Retardation magnification as corollary to apparent superluminal motion

Consider a relativistically moving rod, i.e., an object for which the light-travel time *across* its extent is negligible compared to that

*along* its extent. The rod is subject to Lorentz contraction, so that its rest-frame length  $\Lambda''$  is related to its length in the observer frame by

$$\Lambda = \Lambda'' / \Gamma, \quad (13)$$

where  $\Lambda$  is inferred from a world-map analysis. For the interpretation of observations, where the observer is sufficiently distant from the moving rod to be able to take a *supersnapshot*, we want to relate the apparent size of the object on the supersnapshot to its actual length in the world map. To clarify terminology, the term “projected size” (symbol  $\Lambda_{\text{proj}}$ ) will be used to mean the size that corresponds to the projected extent as measured on the supersnapshot, while the term “apparent size” ( $\Lambda_{\text{app}}$ ) is the size that is inferred from the projected size by deprojecting with the line-of-sight angle  $\theta$ , i.e.,  $\Lambda_{\text{proj}} = \Lambda_{\text{app}} \sin \theta$ . From the constancy and finite value of the speed of light,

$$\Lambda_{\text{app}} = \frac{\Lambda}{1 - \beta \mu} \quad (14)$$

$$= \mathcal{M} \Lambda, \quad (15)$$

where I have defined a magnification

$$\mathcal{M} = (1 - \beta \mu)^{-1}. \quad (16)$$

Substituting eq. (13) recovers the well-known relation

$$\Lambda_{\text{app}} = \delta \Lambda''. \quad (17)$$

(e.g., Ghisellini 2000, eqn. [12]). Equivalently,

$$\Lambda_{\text{proj}} = \delta \Lambda'' \sin \theta \quad (18)$$

$$= \frac{\Lambda \sin \theta}{1 - \beta \mu} \quad (19)$$

$$= \mathcal{M} \Lambda \sin \theta \quad (20)$$

Not by coincidence, the projected velocity  $v_{\text{proj}}$  (usually called “apparent transverse velocity”) in apparent superluminal motion is related to the actual velocity  $v$  by exactly the same magnification factor that relates the projected length to the actual length:

$$\begin{aligned} v_{\text{proj}} &= \frac{v \sin \theta}{1 - \beta \mu} \\ &= \mathcal{M} v \sin \theta. \end{aligned}$$

From eqs. (14), (18) and (19), we can read off all the relevant implications for the interpretation of supersnapshots:

(i) For an approaching rod with  $\mu > 0$ ,  $1 - \beta \mu < 1$  and therefore  $\mathcal{M} > 1$  for any value of  $\beta$ . Thus, the *apparent*, deprojected length  $\Lambda_{\text{app}}$  of a relativistic approaching object is always greater than its observer-frame length  $\Lambda$  as inferred from a world map. In other words, **in a supersnapshot, any approaching relativistic object appears magnified compared to its actual observer-frame size**. Only for  $\theta = 90^\circ$ ,  $\mu = 1$  and  $\Lambda_{\text{proj}} = \Lambda'' / \gamma = \Lambda$ , and the Lorentz contraction of a thin rod becomes observable.

(ii) The projected length  $\Lambda_{\text{proj}}$  is always less than or equal to the rest-frame length  $\Lambda''$ . The limiting case  $\Lambda_{\text{proj}} = \Lambda''$  occurs for  $\mu = \beta$ , which implies  $\delta = \gamma$  and  $\sin \theta = 1/\Gamma$ . In this case, the “projected” appearance of the rod in a supersnapshot is identical to the view of an observer looking at the rod from  $90^\circ$  in its own rest frame, without any Lorentz contraction. This fact was already derived at the end of §1.1, there based on eq. (2).

The second point implies that it is possible to constrain the orientation and speed of a moving relativistic object if its rest-frame size is known. In the case of jets, this may be possible if jet features are

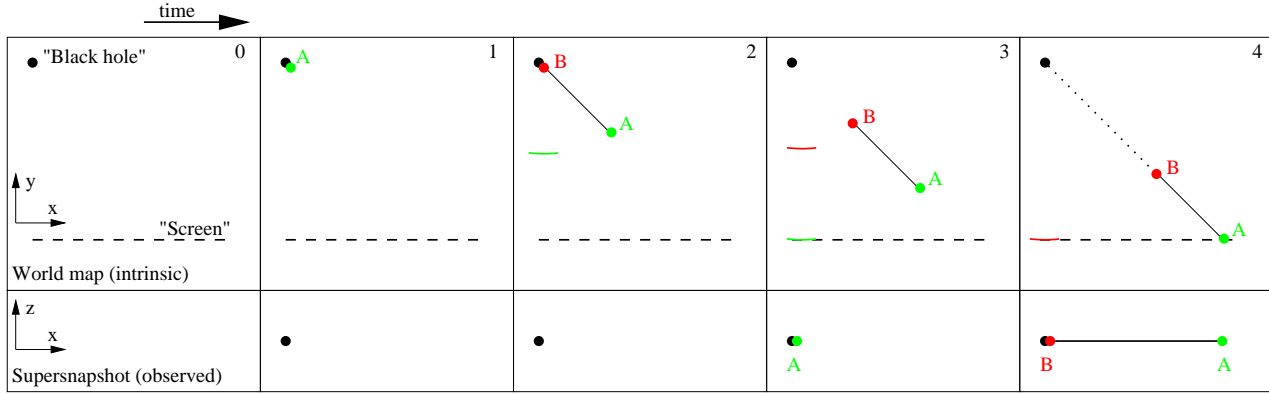


**Figure 1.** Illustration of retardation magnification and hiding, showing a sequence of events in which a relativistically moving “blob” is emitted by some source (e.g., an accretion disk around a black hole), and the picture recorded by a distant observer at the corresponding time. The upper frames give the *world map* in the  $(x, y)$  plane with the true locations of all events; for an infinite speed of light, the world map corresponds to the “top view” of the events as seen by an observer at  $90^\circ$  to the blob’s direction of motion. The lower frames give the *supersnapshot*, the image projected onto the  $(x, z)$  plane as recorded by a distant observer looking along the  $+y$  axis by means of simultaneously arriving photons, i.e., photons that are crossing the dashed “screen” line simultaneously. Panel (0) shows the setup, with the black dot marking the location of the source (“black hole”) ejecting the relativistic blob. (1) The front end “A” of the blob is ejected. (2) The rear end “B” of the blob is ejected, and at the same location as “A” was in frame (1). “A” itself has travelled some distance from the black hole. The curved line illustrates the current location of the wavefront by which the observer will later imply that “A” has been ejected. (3) The wavefront from the ejection of the front end “A” reaches the “screen” location and appears on the observer’s picture. The second wavefront carrying the information about the ejection of “B” is lagging behind. (4) The light from the ejection of the rear end “B” reaches the screen location. At the same time, the front end “A” crosses the screen location. Therefore “B” and “A” appear at the shown locations on the supersnapshot. The separation B–A on the supersnapshot is greater than it is in the world map, and the observer records a magnified image of the blob. If any further material is ejected after “B” (and hence occupied the region indicated by the dotted line), it will not yet be visible to the observer. Hence, the apparent magnification of the blob’s extent implies that any further ejections will be unobservable until the light emitted by them has had time to reach the observer, thus (temporarily) being hidden from view.

known to have a certain ratio of length to width, since the width is not affected by the beaming.

Figure 1 gives a more intuitive illustration of why distant relativistic objects appear magnified in a supersnapshot compared to their true observer-frame extent. As in apparent superluminal motion, the cause of this effect is the time delay between light signals reaching the observer from the end of the object that is closest to the observer and those from the end of the object furthest from the observer. Therefore, I call this effect *retardation magnification*. In analogy to the first point above, any relativistic object’s apparent velocity is *always magnified* compared to its true velocity, without necessarily appearing to be superluminal.

### 2.1.2 Retardation hiding in astrophysical jets

For astrophysical jets, however, there is a catch: jets are produced by accretion disks around a compact object (“core”; for active galactic nuclei, the compact object is a black hole, and similar jets are launched from accretion disks around black holes [Liebovitch 1974, e.g.], neutron stars and white dwarfs in X-ray binaries and novae [see Fender, Belloni & Gallo 2004, e.g.]), and they terminate in a “hot spot” (this can be a shock terminating an FR II jet, or a flaring point at which an FR I jet decelerates substantially). Both are moving through the observer frame much more slowly than the jet material itself. Hence, the apparent size of any jet feature cannot be larger than the separation between the core and the hot spot.

Thus, if jet features appear magnified, it means that not all of the features that are actually *present* in the observer frame can be *visible simultaneously* to the observer, as the total apparent length would then need to be larger than the actual separation between core and hot spot. Hence, the magnification implies that parts of the jet are hidden from the observer’s view. This retardation *hiding* occurs because light signals from the further end of the jet have not

yet had time to reach the distant observer, even though they have already emerged from the core. As the object appears magnified by a factor  $\mathcal{M}$ , it follows that only a fraction  $1/\mathcal{M} = 1 - \beta\mu$  of the object is visible; since time delays are greater for the parts of the object that are further from the observer, the visible part of the jet is that closest to the observer, and the hidden part is that furthest from the observer. Figure 2 shows the visible fraction as function of Lorentz factor and line-of-sight angle. Figure 3 illustrates which parts of a relativistic rod are visible to a distant observer.

The relativity-textbook analogue would be a relativistic train emerging from one tunnel and disappearing into a second one. If the distance between the end of one tunnel and the beginning of the second one is sufficiently short, a distant observer looking at the train from a small angle to the train’s direction of motion will observe fewer railway carriages between the two tunnels than actually fit between them as judged by observers creating a world map.

The magnification obviously applies to blobs, as their outlines are at rest in the *fluid* frame. However, it also applies to individual fluid elements that make up a “jet” feature whose outline is at rest in the *observer* frame. Hence, a given section of an approaching jet actually *contains* more fluid elements than are *visible* simultaneously to an observer. This is another way of deriving that eq. (12) is always the correct volume transformation for supersnapshots, even in the jet case.

The discussion so far has dealt exclusively with 1-dimensional rods, with negligible light travel time in the direction transverse to the direction of motion compared to the light travel time along the direction of motion. This situation does not apply to features of real astrophysical jets, which have comparable extent along and across the direction of motion. The next section illustrates the effect of light-travel delays across a relativistically moving object.

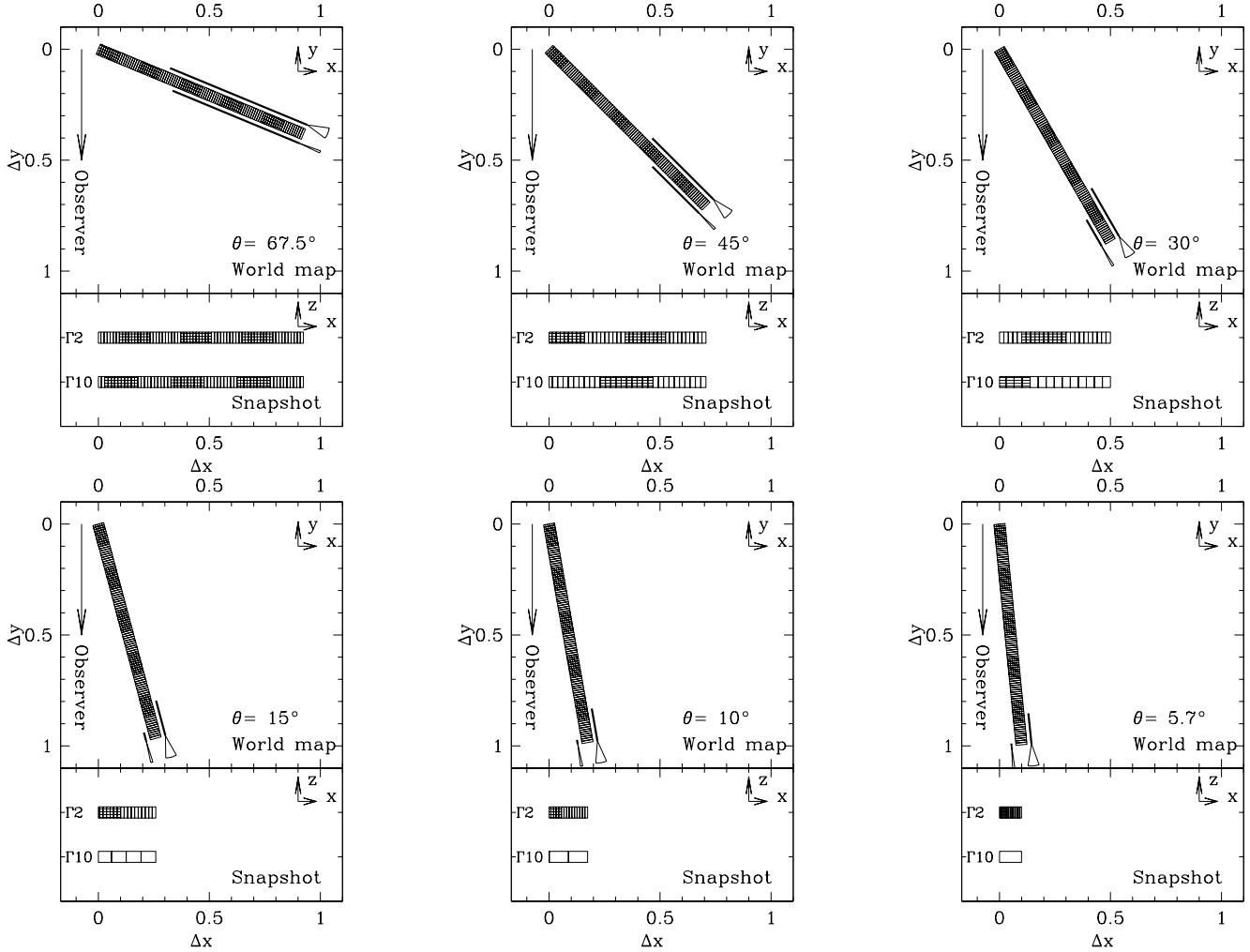


**Figure 3.** Visual appearance of a relativistic rod with features that are fixed in the object’s rest frame (i.e., 1-dimensional blobs), for different line-of-sight angles  $\theta$  and Lorentz factors. As in Fig. 1, the upper panel in each plot shows a “top view world map”, while the lower panel shows the appearance of the jet in a supersnapshot taken by an observer at  $y = -\infty$ . The solid bars above and below the jet in the upper panels indicate the fraction  $1 - \beta\mu$  of the jet that is visible to the pole-on observer, above the jet for  $\Gamma = 2$  (longer bar) and below the jet for  $\Gamma = 10$ . Those photons arriving at a projected position just next to the core were emitted by jet material adjacent to the inner end of the bar at the time when it was just next to the core. All parts of the jet that are closer to the core are not yet visible because the photons from those parts of the jet have not yet had time to reach the observer. The sectors at the ends of the solid bars indicate the relativistic beaming cone of half-opening angle  $\Gamma/2$ ; for the angles and Lorentz factors shown here, only the jets with  $\Gamma = 2$  at angles  $\theta \leq 15^\circ$  have their fluxes enhanced by beaming, while the remainder have their fluxes significantly suppressed by beaming.

## 2.2 Ray-tracing simulations of supersnapshots

To give a visual illustration of the difference between a world map and a supersnapshot, this section contains images of the same emitting regions, once in the world map view, identical to what would be seen if the speed of light was infinite, and once in a supersnapshot view, appropriate for astronomical observations. As just noted, the discussion in the preceding section applies directly to “blob” features, whose outline is at rest in the fluid frame, but also to individual fluid elements making up a “jet” feature, whose outline is at rest in the observer frame. The main difference between a blob and a jet for the ray-tracing images is that the *outline* of blobs experiences the magnification effects. By contrast, the outline of stationary jet features does not get magnified and behaves according to our intuition, which is formed by observing bodies moving at velocities much less than the speed of light. Hence, this section concentrates on the aspect of how the observed (projected) and true geometry of

objects in supersnapshots are related, including the question how to infer the volume of a relativistic object from a supersnapshot.

The discussion here and in the entire the paper is restricted to optically thin objects. The effects of relativistic beaming on flux measurements and quantities derived from them will be examined in the following section.

Figures 4 and 5 shows some simple ray-tracing pictures illustrating the difference between world map and supersnapshot for blobs, and the different projection properties for relativistically moving and stationary features. The following points about observations blobs or jets can be inferred from Figs. 4 and 5:

(i) As expected from Penrose (1959), blobs that are spherical in their rest frame are always observed as spherical blobs, even though they are in fact lens-shaped in the observer frame (due to the Lorentz contraction along the direction of motion). They are still magnified in the supersnapshot, but the magnification is now *along* the line of sight; this is why their observer-frame volume still

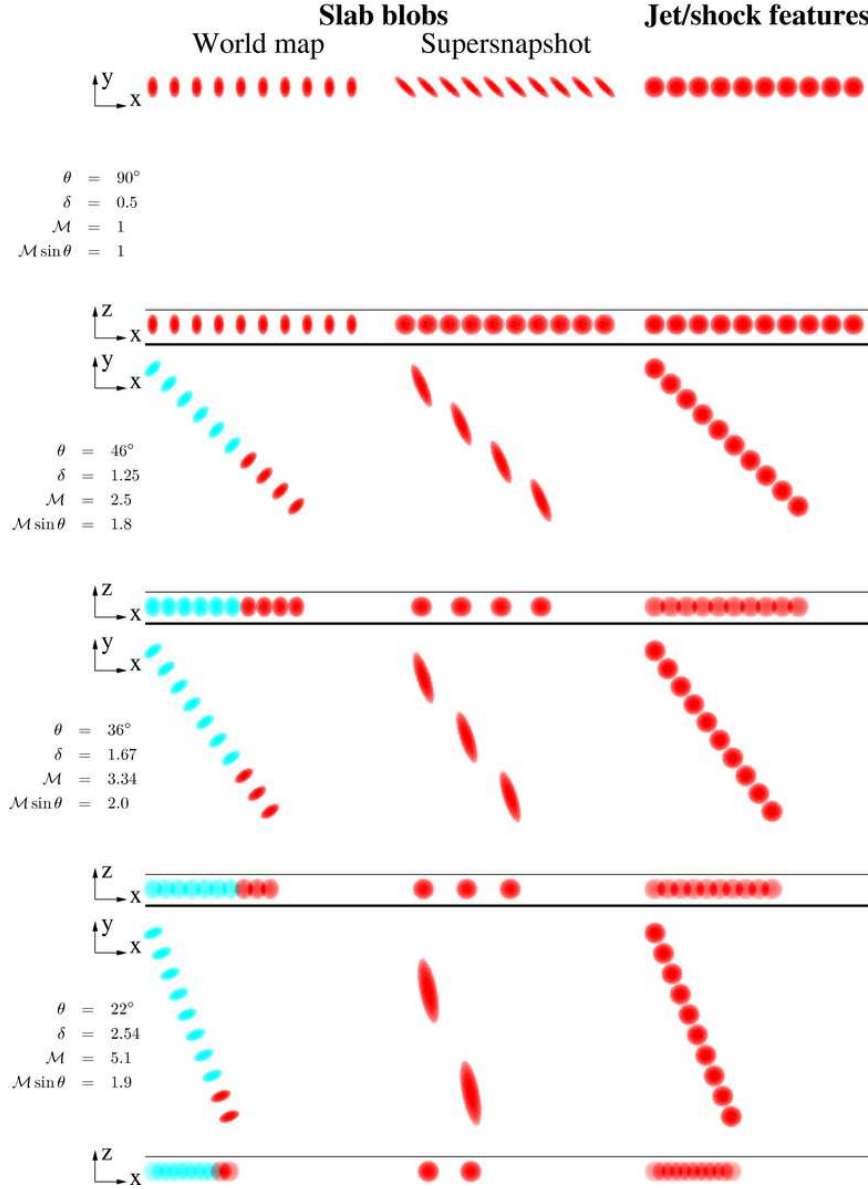


**Figure 4.** World maps and supersnapshots of spherical, optically thin blobs and stationary jet features, with the fluid moving with Lorentz factor  $\Gamma = 2$  at the line-of-sight angles as shown. The two leftmost columns show blobs which are spherical in their own rest frame, the right-hand column shows spherical jet features. The observer is located at  $y = -\infty$ , and blobs that are visible to the observer are shown in red, while blobs that are hidden to the observer are shown in cyan. As in previous figures, there is a panel each for a “top view” and the projected appearance in the plane of the sky; in the case of the “supersnapshot”, both projections include light-travel delays towards the observer, i.e., photons originating at larger  $y$  values left the source at progressively earlier times. For the “supersnapshot” and the “jet” column, the projection onto the plane of the sky is identical to the supersnapshot obtained by a distant observer (for the jet case, it is assumed that the jet is much older than the light travel time difference from the furthest to the nearest feature); for the “world map” column, the projection on the plane of the sky is what *would* be seen if the speed of light was infinite. The world map shows where the emitting material actually *is*, while the supersnapshot shows what is *observed*. The salient points about this figure are: (1) spherical blobs always appear as spherical blobs, but their true observer-frame shape is ellipsoidal; moreover, spherical blobs are magnified *along* the line of sight, retaining the orientation-dependent volume  $V_{\text{app}} = \delta V''$ , but the projection onto the plane of the sky makes this effect unobservable as far as the shape of the object is concerned; (2) while the *shape* of the spherical blobs is unaffected by changes in  $\delta$ , their *spacing* is affected; the projected length of the entire sequence of blobs is the same in the supersnapshot and the world map, but taken up by fewer blobs in the snapshot than there actually are; therefore, some of the blobs are hidden (the hidden blobs are shown in cyan). Thus, (3) the projected appearance of jets and blobs behaves differently as the line-of-sight angle is reduced: jet features move closer together and begin to overlap as the line of sight passes through multiple features, while blobs appear to move further apart.

scales as  $V_{\text{app}} = \delta'' V''$ , even though their projected appearance is identical to their rest-frame appearance.

(ii) The observed *shape* of spherical blobs is not affected by changes in the line-of-sight angle, and hence the Doppler factor; however, their *spacing* changes by a factor  $\delta''$  with respect to their

rest-frame spacing, by  $\mathcal{M}$  with respect to their true observer-frame spacing, resulting in an observed projected spacing of  $\mathcal{M} \sin \theta$  times their true observer-frame spacing. Thus, relativistic blobs (and relativistic objects in general) behave very unintuitive under changes of the observation angle – the closer the line-of-sight an-

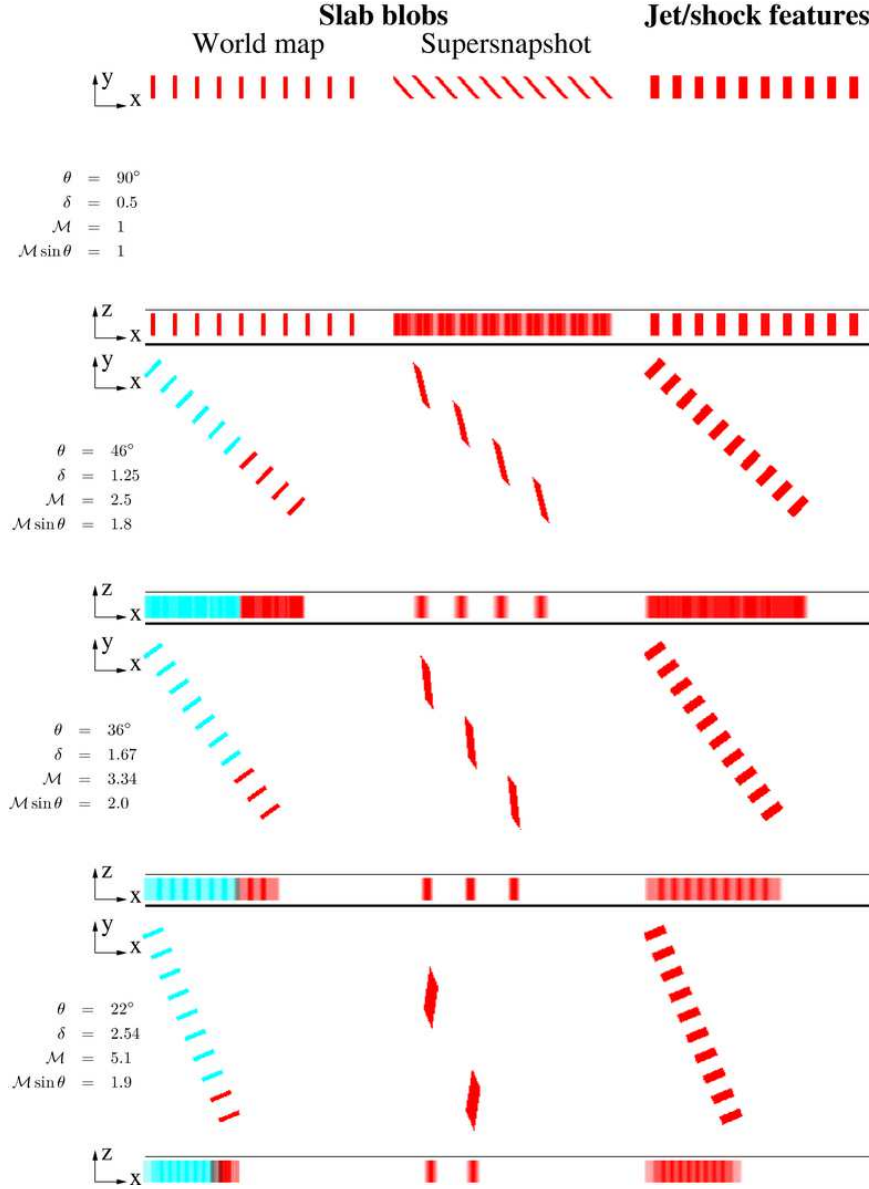


**Figure 5.** As Fig. 4, but with slab features of rectangular cross-section. In the slab geometry, the change of the blob-frame line-of-sight angle is seen clearly, because the projected appearance now varies with that angle: at observer-frame line-of-sight angles greater than the critical angle given by  $\sin \theta = 1/\Gamma$  (corresponding to the “beaming cone” half-opening angle), i.e.,  $\theta = 30^\circ$  for  $\Gamma = 2$ , even approaching blobs are seen from behind in their own rest-frame, and only at line of sight angles  $\theta < 30^\circ$  are the jet features seen from the front. In fact, for a wide range of angles, the features are seen nearly side-on in their own rest frame (compare Bicknell & Begelman 1996). As in the spherical-blob case, fewer and fewer blobs are visible for smaller values of  $\theta$ , and the projected spacing of the knots remains constant over the same range of angles where the knots are seen roughly edge-on.

gle is to the critical angle given by  $\sin \theta = 1/\Gamma$  to the direction of motion, the further they appear to be apart.

(iii) By contrast, stationary spherical jet features behave as expected by our everyday intuition, with smaller projected spacings between individual features for smaller line-of-sight angles.

(iv) The geometry of individual blobs (spherical vs. slab) does not affect *how many* of the blobs are seen, or their total beamed luminosity, but it does affect how the *projected appearance* of individual blobs varies with line-of-sight angle.

The figures do not consider moving shocks, features which are at rest neither in the frame of the observer nor in that of the fluid. However, their projected shape as function of Doppler factor is identical to the projected shape of blobs, i.e., it is governed by the

shock’s Doppler factor  $\delta'$ . The fluid’s emissivity in the observer frame, on the other hand, is governed by the fluid’s Doppler factor  $\delta''$ .

### 3 RELATING OBSERVED AND REST-FRAME QUANTITIES IN JET OBSERVATIONS

Beaming formulae have been given in numerous places in the literature. The usual approach is one that considers a *fixed source volume* and then determines the changes in the received flux density, surface brightness etc. resulting from changes in the Doppler factor, i.e., the line-of-sight angle and Lorentz factor. However, in



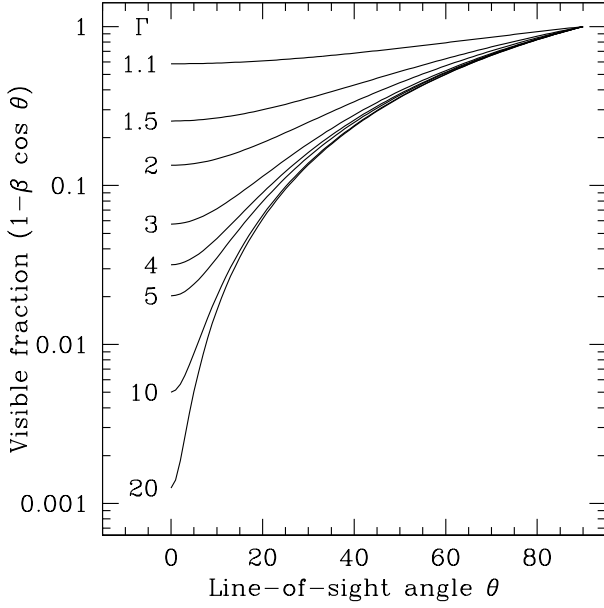


**Figure 2.** Visible fraction of a jet, or other relativistically moving body emerging from a stationary one and disappearing into another stationary one, on a *supersnapshot*, as function of the angle  $\theta$  between the observer's line of sight and the jet's direction of motion, for different Lorentz factors  $\Gamma$  as given. The visible fraction is the inverse of the magnification factor  $\mathcal{M} = (1 - \beta\mu)^{-1}$  defined in the text. Relativistic flux beaming affects the detectability of jets; for  $\Gamma \ll 1$ , the visible fraction of a jet at the critical beaming angle  $\theta \approx 1/\Gamma$  is given by  $5/(8\Gamma^2)$ ; as the jet becomes significantly de-beamed for larger line-of sight angles, this is the maximum visible fraction of the jet material in a relativistic jet.

astronomical observations, it is not the *source* volume that is fixed, but the source's *projected appearance* in the supersnapshot. The fact that the source volume differs when deprojecting the observed appearance with different line-of-sight angles is not considered often in the beaming literature. It is therefore worthwhile to restate the beaming prescriptions for both directions, inferring changing observables for fixed source properties, and changing source properties from fixed observables. As above, the equations assume optically thin, isotropic emission with a power-law emissivity  $j_\nu \propto \nu^\alpha$  that is constant within the emitting region.

### 3.1 Beaming and de-beaming blobs

In the case of a blob, the pattern frame is identical with the fluid frame, so that  $\delta' = 1$  and  $\delta''$  is the relevant Doppler factor. To get observed quantities in terms of source parameters, we need to specify a geometry for the emission region. I consider simple spherical emission regions as well as “slab”-shaped regions of either square or circular cross-section.

#### 3.1.1 Flux beaming of blobs

The beamed total flux density of a blob is given by

$$S_\nu(\nu) = d_L^{-2} \delta''^{3-\alpha} j''_{\nu''}(\nu) V'', \quad (21)$$

where emissivity and source volume are held fixed in the fluid rest frame. The beamed bolometric luminosity is obtained by integrat-

ing  $S_\nu$  over the appropriate range of *rest-frame* frequencies, leading (after substitution using eqs. 7 and 8) to

$$L = \delta''^4 L''. \quad (22)$$

In general, the beaming properties of bolometric quantities are obtained from the frequency differentials by adding  $1 + \alpha$  to the exponent of the Doppler factor, and the exponent to the Doppler factor of beamed bolometric quantities does not contain any spectral-shape parameter such as  $\alpha$ .

#### 3.1.2 Surface brightness beaming of blobs

Surface brightness beaming is important because the detectability of jet features in optical and radio observations is determined by their peak surface brightness, not by their total flux. The observed surface brightness is given by the rest-frame volume emissivity integrated along the observer's line of sight after rotation into the rest frame.

**3.1.2.1 Spherical blobs** For a spherical blob, the beamed surface brightness is  $\delta''^{3-\alpha}$  times the surface brightness that would be perceived by an observer at rest with respect to the blob, but at the same distance. Since the surface brightness of a spherical blob varies according to the different length of the line of sight as function of sky coordinates, I do not give an explicit formula here.

**3.1.2.2 Slab blobs** For a slab blob with square cross-section of side length  $w$ , the observed surface brightness far enough from the edges is independent of sky coordinates and given by

$$I_\nu = \frac{\delta''^{2-\alpha}}{\sin \theta} j''_{\nu''}(\nu) w. \quad (23)$$

Ignoring edge effects is appropriate for slab blobs with length:width ratios greater than about 2. The same expression applies to the surface brightness along the projected axis of a cylindrical blob with observed diameter  $w$ , and the scaling of observed surface brightness with the beaming parameters  $\Gamma, \theta$  applies to the entire cylindrical blob.

#### 3.1.3 Inferring the rest-frame properties of blobs

Equations (21) and (22) by themselves give the dependence of received flux and inferred luminosity on observation angle and Lorentz factor. In order to infer rest-frame quantities such as  $j''$  from observations, it is necessary to infer the rest-frame volume from the source's projected appearance. The prescription for this depends on source geometry.

**3.1.3.1 Spherical blobs** As discussed above, a spherical blob will appear as the same spherical blob to any observer, including the rest observer. Hence, the rest-frame volume is simply  $V'' = 4/3\pi R^3$ , where  $R$  is the observed radius of the blob. This apparently contradicts eq. (12), but there is in fact no contradiction, as can be seen from Fig. 4: the  $(x, y)$  view of the “supersnapshot” column shows that for  $\delta > 1$ , the (unobservable) “observer-frame volume” of a spherical blob has a larger extent *along* the line of sight than can be inferred from its projected appearance, and a smaller one for  $\delta < 1$ . Thus, the rest-frame emissivity of the material is given by

$$j''_{\nu''}(\nu) = S_\nu(\nu) d_L^2 \frac{\delta''^{-3+\alpha}}{4/3\pi R^3}. \quad (24)$$

**3.1.3.2 Slab blobs** Next, I consider a slab-shaped blob with square or circular cross-section  $A$ , i.e., a blob whose intrinsic size perpendicular to the direction of motion can be inferred directly from its transverse angular size in the plane of the sky. The rest-frame length of the slab can be inferred from the projected length  $\Lambda_{\text{proj}}$  and the fact that our line of sight crosses the blob in its rest frame at an angle given by eq. (2), i.e.,  $\Lambda'' = \Lambda_{\text{proj}}/(\delta \sin \theta)$ . Thus,  $V'' = A \Lambda_{\text{proj}}/(\delta \sin \theta)$  and

$$j''_{\nu''}(\nu) = S_{\nu}(\nu) d_L^2 \frac{\delta''^{-2+\alpha} \sin \theta}{A \Lambda_{\text{proj}}}, \quad (25)$$

again ignoring edge effects.

Comparing to the relation between observed flux and rest-frame volume emissivity, eq. (21), it appears to be a contradiction that eq. (25) has a different scaling with Lorentz factor and observation angle. The difference arises because eq. (21) applies to observations of the same *source* from different directions ( $V''$  is kept fixed), while eq. (25) describes the situation where the *observables* are kept fixed, so that different line-of-sight angles correspond to different inferred values for  $V''$ . The decisive aspect that is often neglected is the length of the sight line across the blob changes due to the relativistic angle aberration (eq. 2), leading to the  $\sin \theta$  term in the final expression. Because of this line-of-sight deprojection, the “de-beaming” formula cannot be expressed as function of the Doppler factor  $\delta''$  only.

## 3.2 Beaming and de-beaming jets

### 3.2.1 Beamed flux density of a jet

The beamed flux density of a jet feature is given by

$$S_{\nu}(\nu) = d_L^{-2} \delta''^{2-\alpha} j''_{\nu''}(\nu) V. \quad (26)$$

This arises simply from integrating the fluid-frame emissivity transformed into the observer frame over the observer-frame volume. Though comparison with the blob case, eq. (21), seems to reveal the usual difference in the exponent of the Doppler factor between “jet” and “blob” case, the expression is multiplied by *different* volumes, fluid-frame  $V''$  for the blob case, observer-frame  $V$  for the jet case, that are at rest in *different* frames. Therefore, merely comparing the exponent of the Doppler factor does not contain the full information about beaming properties of blobs versus jets.

### 3.2.2 Beamed surface brightness of a slab jet

If the emitting volume is a slab jet with transverse width  $w$ , the volume of a section with projected length  $\Lambda_{\text{proj}}$  is just  $V = w^2 \Lambda_{\text{proj}}/\sin \theta$ . Hence, the observed surface brightness of such a slab jet is

$$I_{\nu} = \frac{\delta''^{2-\alpha}}{\sin \theta} j''_{\nu''}(\nu) w, \quad (27)$$

This is identical to the beamed surface brightness of a slab *blob* (eq. 23), as it must, because a continuous jet can be considered as a section of a long blob.

### 3.2.3 Inferring rest-frame properties of jets

Asking about the “rest-frame” volume of a jet feature is not directly meaningful, since the outline of the jet feature is at rest in the observer’s frame, while the emitting fluid is not, so there isn’t a single frame in which both the fluid and its outline are at rest. However,

by substituting eq. (12), we can of course express eq. (26) in terms of the volume  $V'' = V/\delta''$  of jet fluid that contributes photons to the observer’s supersnapshot, obtaining the same expression as for the “blob” case, eq. (21), and hence also the same expression for the relation between observer-frame and fluid-frame bolometric luminosity, eq. (22).

If the supersnapshot nature of astronomical observations were ignored, an alternative definition of “fluid-frame luminosity” of a jet could be derived by noting the following: according to the world map of an observer at rest in the fluid frame, the volume of the jet is *contracted*. Hence,  $V'' = V/\Gamma$  and the fluid-frame bolometric luminosity would be given by  $L'' = 4\pi j'' V'' = L/(\delta''^3 \Gamma)$  — i.e., exactly the opposite scaling of  $V''$  and hence  $L''$  with  $\Gamma$  from that given by Stawarz et al. (2003, eqn. A3). The reason for this apparent contradiction, and that it is only apparently a contradiction, is again that result of a relativistic experiment depends on what is held constant in which frame (compare Appendix A). All that matters for jet observations is the supersnapshot with constant photon arrival times.

Equation (26) of course correctly describes the dependence of the received flux for a fixed jet feature when varying the fluid’s Lorentz factor and the line-of-sight angle. As long as we infer the correct observer-frame  $V$  from the fixed apparent size of a jet feature as function of the unknown fluid Lorentz factor and the line-of-sight angle, we can infer the fluid-frame emissivity by inverting that equation.

For a spherical jet feature, the observer-frame volume can of course be inferred directly from the projected radius  $R$  of the sphere, leading to

$$j''_{\nu''}(\nu) = S_{\nu}(\nu) d_L^2 \frac{\delta''^{-2+\alpha}}{4/3\pi R^3}. \quad (28)$$

For a “slab” feature, we can measure its cross-sectional area  $A$  and assume some rotational symmetry. For fixed projected length  $\Lambda_{\text{proj}}$ , the deprojected length is then just  $\Lambda_{\text{proj}}/\sin \theta$ , so that the relation between emissivity and observed flux of a jet section is

$$j''_{\nu''}(\nu) = S_{\nu}(\nu) d_L^2 \frac{\delta''^{-2+\alpha} \sin \theta}{A \Lambda_{\text{proj}}},$$

again ignoring edge effects, i.e., assuming a length:width ratio of greater than about 2. This expression is identical to equation (25), the relation between observables and rest-frame emissivity for a slab-shaped *blob* of fixed projected size but unknown  $(\Gamma, \theta)$ . In other words, our lack of knowledge about jet orientation and Lorentz factor affects elongated slab-shaped blobs and jets in exactly the same way.

However, for a *sphere* of fixed observed radius  $R$ , the inferred fluid-frame emissivity is different by one power of  $\delta$  depending on whether we are considering a spherical blob or a spherical jet feature (compare eqns. 28 and 24). This difference between the beaming of an elongated and a spherical blob arises because a spherical blob in effect becomes magnified *along* the line of sight, while a slab blob appears magnified *in the plane of the sky*, as discussed in §3.1.3 above (again compare Figure 4). The elongation *along* the line of sight is unobservable in the projection on the plane of the sky. Thus, in the special case of spherical features, there *is* a difference between “jet” and “blob” de-beaming.

## 3.3 The minimum-energy magnetic field of beamed sources

A synchrotron source, such as the radio jet of an active galactic nucleus, is powered by energy stored either in its magnetic

field or in relativistic particles. As first pointed out by Burbidge (1959), there is a minimum to the total energy in particles and fields that is required to power a given observed synchrotron luminosity. This minimum can be parameterized in terms of the magnetic field strength at the minimum energy density, which is often used as “the minimum-energy magnetic field estimate”.

Further derivations and ready-to-use formulae for non-relativistic sources are given by Pacholczyk (1970), Longair (1994) and Miley (1980). Beck & Krause (2005) have offered some constructive criticism on this so far well-established formalism, in particular regarding the unknown ratio  $K$  of total energy in relativistic protons and electrons. Harris & Krawczynski (2002) and Stawarz et al. (2003) have presented detailed derivations of minimum-energy estimates in the rest frame of relativistic jets, but reached slightly different conclusions. Armed with the knowledge from the preceding sections, we can now reconsider the question of the correct de-beaming of minimum-energy magnetic field estimates.

As noted above, for the case of a “jet” geometry, the rest frame of the fluid cannot be identified with the rest frame of the “source”, as the source volume is *fixed* in the observer frame, while the beaming is determined by the Lorentz factor at which the fluid is *moving* through the observer frame. The same applies for shocks. However, as extragalactic jets are assumed to be close to ideal MHD conditions, the rest frame of the fluid is also the rest frame of the magnetic field, and the frame in which the electron energy distribution is assumed to be isotropic. Thus, whether we are considering blobs or jets, the fluid rest frame is the frame in which the minimum-energy field needs to be calculated in order to satisfy the underlying assumptions. As before, the emission is assumed to be optically thin emission with spectral shape  $j_{\nu''} \propto \nu''^\alpha$  and constant emissivity throughout the emission region.

In the absence of beaming, the expression for the minimum-energy field in terms of quantities in the rest frame of the fluid (double primes) is

$$B_{\min}''^{7/2} \propto \frac{\nu_2''^{1/2+\alpha} - \nu_1''^{1/2+\alpha}}{\nu_2''^{1+\alpha} - \nu_1''^{1+\alpha}} \frac{L''}{V''}, \quad (29)$$

where the synchrotron spectrum extends over the rest-frame frequency interval  $(\nu_1'', \nu_2'')$ ; the first fraction is from the function  $\tilde{c}$  from Pacholczyk (1970, eqn. 7.8). As pointed out above, neither the rest-frame volume  $V''$  nor the observer-frame volume  $V = \delta V''$  is fixed by observations when the line-of-sight angle is unknown, but it is the projection of the source on the plane of the sky that needs to be kept fixed. Nevertheless, it is instructive to compare the minimum-energy field as function of  $\Gamma$  and  $\theta$  inferred for fixed source volume to that inferred for fixed projected appearance. Hence both will be rederived here, beginning with the fixed-source case (§3.3.1), followed by the fixed-projection case §3.3.2. Their direct juxtaposition illustrates why differing opinions have arisen in the literature about how minimum-energy parameters scale with Doppler factor.

### 3.3.1 Minimum-energy parameters for fixed source volume

**3.3.1.1 Blob case** For a blob, the source volume is at rest in the fluid frame, therefore  $V''$  is unambiguous, and the beamed minimum-energy field is obtained from eq. (29) by inserting  $L'' = \delta''^{-4} L$ ,  $V'' = \delta''^{-1} V$ , and  $\nu_{1,2}'' = \delta''^{-1} \nu_{1,2}$ . Hence,  $B_{\min}''^{7/2} \propto \delta''^{-5/2}$  and

$$B_{\min}(\delta'') = B_{\min}(\delta'' = 1) \delta''^{-5/2}. \quad (30)$$

This is identical to equation (A8) of Stawarz et al. (2003), which implies that their expression applies to the fixed-volume case considered here, not the fixed-observable case relevant to the interpretation of observations. It is different from equation (A7) of Harris & Krawczynski (2002) because those authors explicitly considered the fixed-observable case for a spherical blob whose rest-frame volume  $V''$  is inferred directly from observables, the case that will be discussed in the following subsection.

**3.3.1.2 Jet case** From the frequency integral of the definition of monochromatic luminosity (eq. 7) and the  $\delta''$ -dependence of the emissivity  $j_\nu$  (eq. 11; also eqn. 2.5 of Lind & Blandford 1985), the bolometric luminosity of a jet section scales with the Doppler factor of the fluid as  $\delta''^3$ . Hence,  $L''/V$  for a jet scales in exactly the same way as  $L''/V''$  for a blob. The Doppler scaling of the frequencies occurring in the  $\tilde{c}$  expression are identical to the blob case. Hence, the expression from eq. (30) is obtained for the jet case also. Again, this is the same result obtained by Stawarz et al. (2003), again because they were implicitly considering the fixed-volume case.

### 3.3.2 Minimum-energy field for fixed observables

This section describes how to infer the rest-frame minimum-energy field from astronomical observations as function of the unknown Lorentz factor and line-of-sight angle (usually only considered in their combination as Doppler factor) in the case relevant to observations, where it is not the source volume that is kept fixed, but the source’s projected appearance. As in §§3.1 and 3.2, the computation of the source volume needs to be done taking into account that changing the Lorentz factor and line-of-sight angle not only changes the Doppler factor, but also the *length of the sight line through the object* due to the relativistic angle aberration (eq. 2). The differences between the formulae presented below and those in the literature arise because the effects of angle aberration are stated here explicitly.

To express the minimum-energy field as function of an observed flux density at some frequency  $\nu_{\text{obs}}$ , assuming a power-law spectrum, one expresses the rest-frame flux density in terms of the rest-frame luminosity

$$S''_\nu(\nu_{\text{obs}}) = \frac{L''}{4\pi d_L^2} \frac{1+\alpha}{\nu_2''^{1+\alpha} - \nu_1''^{1+\alpha}} \nu_{\text{obs}}^\alpha. \quad (31)$$

Substituting into eq. (29), one obtains

$$B_{\min}''^{7/2} \propto S''_\nu(\nu_{\text{obs}}) \nu_{\text{obs}}^{-\alpha} \frac{\nu_2''^{1/2+\alpha} - \nu_1''^{1/2+\alpha}}{V''}. \quad (32)$$

As above (§3.1), the transformation properties for fixed observables depend on the source geometry.

Before considering this expression for different source geometries, it is important to note that the  $\nu_{\text{obs}}$  term in this and the derived expressions does *not* scale with the Doppler factor, since it is explicitly the fixed observing frequency. The effect of observing the rest-frame spectrum at a Doppler-shifted frequency and hence at a different amplitude is already accounted for by the  $-\alpha$  ( $K$ -correction) term that appears in the exponent of the Doppler factor multiplying the observed flux density. In other words, even when  $B_{\min}$  is expressed in terms of  $S_\nu(\nu_{\text{obs}})$ , which scales as  $\delta''^{3-\alpha}$ , the spectral index  $\alpha$  does not appear in the exponent of  $\delta''$  in the final expression for the minimum-energy field, or the minimum energy content, because the minimum-energy field depends on *bolometric* quantities and all  $K$ -correction terms drop out again. This is also relevant for deriving the boosted version of the yet-lower limit to

the energy content of a synchrotron source that Longair (1994, p. 296, eqn. 19.29) obtains by setting  $\nu_1 = \nu_{\text{obs}}$  in eq. (31) and neglecting the other frequency integration limit. This substitution has to be done in the Doppler-boosted expressions for the appropriate geometry, as derived below. Hence, it would not be correct to set  $\nu'' = \nu_{\text{obs}}$  in eq. (32) and apply the boosting afterwards; in other words, the beamed version of eq. (19.29) of Longair (1994) *cannot* be obtained simply by inserting Doppler factors into it. Once more, the correct boosting transformation needs to be applied not only to the *integrand*, but also to the *integration boundaries*, and care has to be taken to do both transformations at the same time.

**3.3.2.1 Spherical blobs** Since relativistically moving spheres are always observed with a spherical outline, the rest-frame volume of a spherical blob can be inferred directly from the observed radius  $R$  as  $V'' = 4/3\pi R^3$ . Substituting this and the appropriate Doppler boosting for flux density (eq. 21) and frequency (eq. 8) into eq. (32) yields

$$B''_{\min}{}^{7/2} \propto S_{\nu}(\nu_{\text{obs}}) \nu_{\text{obs}}^{-\alpha} \frac{\nu_2^{1/2+\alpha} - \nu_1^{1/2+\alpha}}{4/3\pi R^3} \delta''^{-7/2}. \quad (33)$$

This implies that  $B''_{\min} \propto \delta''^{-1}$ , precisely eq. (A7) of Harris & Krawczynski (2002), and reassuring since they explicitly considered only this special case of a spherical blob. However, hardly any of the currently known jets has knots with morphology that accurately can be described as spherical.

**3.3.2.2 Slab or cylindrical blobs** As discussed above, if a slab-shaped or cylindrical blob with intrinsic length:width ratio of greater than 2 is observed to have a projected length (image extent)  $\Lambda_{\text{proj}}$  and cross-sectional area  $A$ , its rest-frame volume is  $V'' = A\Lambda_{\text{proj}}/\delta'' \sin \theta$ . Performing the corresponding substitutions into eq. (32), one obtains

$$B''_{\min}{}^{7/2} \propto S_{\nu}(\nu_{\text{obs}}) \nu_{\text{obs}}^{-\alpha} \frac{\nu_2^{1/2+\alpha} - \nu_1^{1/2+\alpha}}{A\Lambda_{\text{proj}}} \delta''^{-5/2} \sin \theta. \quad (34)$$

The scaling of rest-frame minimum-energy field with the unknown Lorentz factor and line-of-sight angle  $\theta$  of such a blob is  $B''_{\min} \propto \delta''^{-5/7} (\sin \theta)^{2/7}$ , i.e., it is not expressible purely as function of the Doppler factor  $\delta''$  because the length of the sight line through the blob scales with  $\sin \theta$ . The scaling differs from that of Harris & Krawczynski (2002) because they considered only spherical blobs, and from that of Stawarz et al. (2003) because they did not consider the fixed-observable case.

**3.3.2.3 Jet case** In the jet case, the appropriate fluid-frame volume  $V''$  is again the volume of fluid that contributes photons to the supersnapshot, rather than the *actual* Lorentz-contracted volume inferred from the world map; hence, the appropriate volume is given by  $V'' = V/\delta''$ . For a jet with cross-sectional area  $A$  and projected length  $\Lambda_{\text{proj}}$ , the observer-frame volume is again  $V = A\Lambda_{\text{proj}}/\sin \theta$ , and hence  $V'' = A\Lambda_{\text{proj}}/\delta'' \sin \theta$  – identical to the slab/cylindrical blob case. Therefore, eq. (34) applies also to continuous jets, analogous to the identical “de-beaming” equations for slab blobs and jets in §§3.1 and 3.2.

**3.3.2.4 An amusing special case** Usually both  $\theta$  and  $\Gamma$  are unknown in jet observations. However, the fact that the jet emission is detectable makes it more likely that the emission is beamed towards the observer than that it is beamed away from the observer. A frequent guessimate that reduces the number of unknown beaming

parameters from 2 to 1 is therefore  $\delta = \Gamma$ , equivalent to  $\mu = \beta$  and  $\sin \theta = 1/\Gamma$ . Substituting this assumption into eq. (34) leads to

$$B''_{\min} \propto 1/\Gamma = \sin \theta.$$

Thus, if  $\delta = \Gamma$ , the true fluid-frame minimum-energy field is given by

$$\begin{aligned} B''_{\min} &= B_{\min}^{(0)} \times 1/\Gamma \\ &= B_{\min}^{(0)} \times \sin \theta, \end{aligned}$$

where  $B_{\min}^{(0)}$  is the minimum-energy field inferred from the observables by neglecting beaming and projection effects and assigning the source a volume  $A\Lambda_{\text{proj}}$ . It also turns out that at fixed  $\theta$ ,  $\delta''^{-5/7} (\sin \theta)^{2/7} \geq 1/\Gamma$ . Hence, the true minimum-energy field at fixed  $\theta$  is always larger than  $1/\Gamma \times B_{\min}^{(0)}$ .

## 4 DISCUSSION AND SUMMARY

In §2, I have illustrated the difference between the *world map* of a relativistic jet, what is actually there, and the *world picture*, or its special case, the *supersnapshot*, that corresponds to what is observable by distant astronomers. For the quantitative interpretation of world pictures in the presence of unknown beaming parameters (Lorentz factor  $\Gamma$  and angle  $\theta$  between the fluid motion and the line of sight), what matters is that the *projected appearance* of the jet is kept fixed and not the *intrinsic volume*. This gives rise to de-beaming formulae that are slightly different from those in the existing literature.

### 4.1 Implications for interpretation of flux and surface brightness of jet features

The most important conclusion for the quantitative analysis of jet observations is that the scaling relations relating rest-frame quantities (volume emissivity, intrinsic source size) to observables (projected source size, surface brightness, total flux) *cannot* be stated as function of the line-of-sight angle and Lorentz factor in a general way, but depend on the details of the source geometry. It is possible to write down explicit scaling relations for certain simple geometries such as spheres and elongated, rotationally symmetric blobs of constant cross-section. For other shapes, such as ellipsoidal blobs or blobs with non-symmetric cross-sections, the projected appearance is affected by edge effects, and additionally by observational effects such as the contrast between the faintest parts of the source and the sky background, as well as the available signal-to-noise level. Edge effects are properly taken into account by the ray-tracing in §2.2, and such ray-tracing modeling of observables is probably the most accurate route to interpreting observations of relativistic objects. Indeed, it is part of the prediction of observables from jet simulations such as those by Aloy et al. (2003), e.g. The work of Swift & Hughes (2008), which explicitly considers the relation between the jet appearance in a supersnapshot and the underlying physical quantities, taking into account the retardation along the line of sight.

## 4.2 Implications for interpretation of morphological information in jet images

Most radio, optical and X-ray maps of relativistic jets (a list of radio jets is given by Liu & Zhang 2002)<sup>2</sup> show a series of well-separated, distinct features usually referred to as “knots”, with diffuse emission linking them. Given that relativistic beaming favours the detection of objects with jets at small angles to the line of sight, and the superluminal motions detected in the cores of many such sources, it is plausible that the jet material itself is still relativistic even at large separations (and indeed, this is required in models accounting for the X-ray emission from powerful radio jets as beamed inverse-Compton scattering of cosmic microwave background photons; see Tavecchio et al. 2000; Celotti et al. 2001 for the original development of the idea, as well as the recent review by Harris & Krawczynski (2006)). However, what is not clear is whether the knots themselves are stationary shock features, or themselves moving relativistically.

Referring to Figs. 4 and 5, the prevalence of well-separated knots in jet images seems to suggest that the knots are moving at least with mildly relativistic Lorentz factors – otherwise, there should be *some* jets observed at small angles (favoured by Doppler boosting) where different knots overlap along the line of sight, washing out any individual morphological features.

In this case, the knots are subject to retardation magnification and hiding (illustrated in Figs. 1 and 3), and we are not seeing *all* of the jet features which are actually present between core and hot spot, but just a small fraction (whose magnitude is given by Fig. 2). An observation of apparent superluminal motion of individual knots would be a direct confirmation that they are moving relativistically, as in the case of parsec-scale knots in VLBI observations. The kiloparsec-scale knots are resolved out in VLBI observations, so that very long-term monitoring programmes at sub-arcsecond spatial resolution are required to make a potential superluminal motion observable.

If jet knots are indeed moving relativistically, the retardation magnification and hiding need to be taken into account when interpreting morphological observables such as the ratio between knot separation and jet width, which is important for addressing the question of the origin of the jets’ morphological features, e.g., whether they arise from instabilities (Hardee 2003) or as manifestation of a stable magnetohydrodynamical configuration (Königl & Choudhuri 1985).

## 4.3 Conclusion

It becomes clear once more that relativistic effects are counter to our non-relativistic intuition, and that familiarity with *world maps*, Lorentz transformations and the resulting phenomena of length contraction and time dilation is not sufficient for interpreting *world pictures*. When considering the beaming properties of quantities expressed in terms of integrals, such as a surface brightness, flux or the minimum-energy magnetic field estimate, one needs to consider the transformation properties both of the integrand and the integration volume. Apparent differences between the beaming properties of “blobs” and “jets” disappear when the same source volume is considered. Finally, the de-beaming of astronomical observations needs to be done not for a fixed source, but for the fixed *projection*

of the source. Doing so resolves some conflicts (again only apparent ones) between different de-beaming formulae in the literature. Given that astronomy provides only world pictures, the concepts first laid out by Penrose (1959) and Terrell (1959) deserve more attention in the interpretation of jet observations.

## ACKNOWLEDGMENTS

This research has made extensive use of NASA’s Astrophysics Data System Bibliographic Services. I am grateful to Herman Marshall for valuable discussions and the impulse to begin this work, and acknowledge fruitful interactions with members of the Fermilab Experimental Astrophysics Group, and the Astronomy group at the University of Southampton. I am particularly grateful to Łukasz Stawarz for detailed feedback in early stages of this work, to Jochen Weller, Rob Fender and Dan Harris for continued discussions, to Arie Königl for helpful comments on the paper – in particular for reminding me of the Lorentz invariance of opacity – and to W.C. Herren for inspiration. I thank the referee, Henric Krawczynski, for his constructive criticism which helped me improve the presentation of this material. The portion of this work carried out at Fermilab was supported through NASA contract NASGO4-5120A and through the U.S. Department of Energy under contract No. DE-AC02-76CH03000. Last but not least, I acknowledge support through an Otto Hahn Fellowship from the Max-Planck-Institut für Astronomie that enabled much of this work to be carried out within the Astronomy Group at the University of Southampton, whose hospitality I enjoyed tremendously.

## APPENDIX A: LORENTZ EXPANSION AND TIME ACCELERATION? A QUESTION OF THE VIEWPOINT

The world-map analysis familiar from physics textbooks shows that relativistically moving objects experience Lorentz contraction and time dilation. The derivation begins with the Lorentz transformations between frames  $\Sigma$  and  $\Sigma''$  with aligned  $x$  and  $x''$  axes and origins coinciding at  $t = t'' = 0$ :

$$t = \gamma(t'' + \beta x'') \quad (\text{A1})$$

$$x = \gamma(x'' + \beta t''). \quad (\text{A2})$$

To show that there is Lorentz contraction of objects at rest in  $\Sigma''$ , one considers two observers at rest in  $\Sigma$  which coincide with opposite ends of the moving object at some fixed  $t$ , e.g.,  $t = 0$ . Solving eq. (A1) for  $t''$  and substituting into eq. (A2) then yields  $x_2 - x_1 = (x_2'' - x_1'')/\gamma$ , i.e., length contraction. Time dilation is obtained by considering a clock at rest in  $\Sigma''$  whose time is read by two different observers in  $\Sigma$ , e.g., one at  $(x, t) = (0, 0)$ , the second at  $(x, t) = (x_1, t_1 = x_1/\beta)$ . The first observer reads  $t'' = 0$  (by convention); setting  $x'' = 0$  in eq. (A1), the second observer reads  $t'' = t/\gamma$  on the moving clock, i.e., infers that a shorter time interval has elapsed in the moving frame than in the observers’ frame and that time is therefore dilated.

However, we can ask our observers to do slightly different experiments. Imagine that there are a large number of clocks in  $\Sigma''$ , and we are told that the clocks are all synchronized in that frame. To investigate the behaviour of time, we ask a single observer to compare the time read on successive clocks that are whizzing past to her own observer-frame clock. In other words, instead of keeping  $x''$  fixed, let us keep  $x$  fixed, and choose the observer at  $x = 0$ . The first clock reads  $t'' = 0$ . If the clocks are separated in  $\Sigma''$  by some

<sup>2</sup> See <http://home.fnal.gov/~jester/optjets/> and <http://hea-www.harvard.edu/XJET/> for lists of optical and X-ray jets.

distance  $l''$ , the second clock, being at  $x'' = -l''$  will reach the observer at  $t'' = l''/\beta$ . At this time, the observer's own clock reads  $t = l''/(\beta\gamma) = t''/\gamma$ ; thus, the observer's clock has advanced less than the moving ones, and time is accelerated instead of dilated. The reconciliation with time dilation is, of course, that the second moving clock did not read  $t'' = 0$  at  $t = 0$ , but already  $t'' = \beta l''$  — the clocks that are synchronized in  $\Sigma''$  are *not* in  $\Sigma$ , simultaneity is relative. Indeed, this setup allows the observers at rest in  $\Sigma$  to infer that *their* clocks are slowed down relative to observers in  $\Sigma''$ : it compares the time interval elapsed on a *single* clock in one frame to the interval elapsed between two *different* clocks in another frame. The individual clock runs slow compared to two different clocks whizzing past it, or that it whizzes past.

We can also derive an alternative length measurement. Assume that the observers know about special relativity, and that the observers in  $\Sigma''$  have placed a clock at the front and rear end of the object whose length the observers in  $\Sigma$  are trying to measure. These observers decide to measure the length by taking into account the relativity of simultaneity, and they do so by noting the position of each clock in their own frame when it shows a fixed time in the *moving* frame,  $t'' = 0$ , say. If the rear clock is at  $x'' = 0$ , it reads  $t'' = 0$  at  $t = 0$  and will be seen by the observer at  $x = 0$ . The front clock is at  $x'' = l''$ , and thus from eq. (A2) it will read  $t'' = 0$  when it has reached the observer at  $x = \gamma l''$ . Hence, the observers in  $\Sigma$  infer that the moving rod has expanded by a factor  $\gamma$  compared to what it is in its own rest frame. Again, this is just the converse of the observers in  $\Sigma''$  measuring the length of an object at rest in  $\Sigma$  and finding that the moving object has contracted.

Thus, observers in either frame can both observe that moving objects appear contracted to them *and* infer that something that is at rest in their own frame will appear contracted to observers in the other frame; similarly, observers can observe clocks in the other frame run slow *and* infer that their own clocks will be observed to run slow by observers in the other frame. The important point is that the outcome of an experiment depends on *which quantity is held fixed in which frame*, and the correct interpretation of apparently contradictory results depends on being clear in the description of the experiment.

## REFERENCES

- Aloy M.-Á., Martí J.-M., Gómez J.-L., Agudo I., Müller E., Ibáñez J.-M., 2003, *ApJ*, 585, L109
- Beck R., Krause M., 2005, *Astronomische Nachrichten*, 326, 414
- Begelman M. C., Blandford R. D., Rees M. J., 1984, *Rev. Mod. Phys.*, 56, 255
- Bicknell G. V., Begelman M. C., 1996, *ApJ*, 467, 597
- Blandford R. D., Königl A., 1979, *ApJ*, 232, 34
- Burbidge G. R., 1959, *ApJ*, 129, 849+
- Celotti A., Ghisellini G., Chiaberge M., 2001, *MNRAS*, 321, L1
- Einstein A., 1905, *Annalen der Physik*, 322, 891
- Fender R. P., Belloni T. M., Gallo E., 2004, *MNRAS*, 355, 1105
- Ghisellini G., 2000, in Casciaro B., Fortunato D., Francaviglia M., Masiello A., eds, *Recent Developments in General Relativity Special Relativity at Action in the Universe*. pp 5—+
- Hardee P. E., 2003, *ApJ*, 597, 798
- Harris D. E., Krawczynski H., 2002, *ApJ*, 565, 244
- Harris D. E., Krawczynski H., 2006, *ARA&A*, 44, 463
- Harris D. E., Krawczynski H., 2007, in *Revista Mexicana de Astronomía y Astrofísica*, vol. 27 Vol. 27 of *Revista Mexicana de Astronomía y Astrofísica Conference Series*, Constraints on the Nature of Jets from KPC Scale X-Ray Data. p. 188
- Jester S., Harris D. E., Marshall H. L., Meisenheimer K., 2006, *ApJ*, 648, 900
- Königl A., Choudhuri A. R., 1985, *ApJ*, 289, 173
- Liebovitch L. S., 1974, *QJRAS*, 15, 141
- Lind K. R., Blandford R. D., 1985, *ApJ*, 295, 358
- Liu F. K., Zhang Y. H., 2002, *A&A*, 381, 757
- Longair M., 1994, *High-energy astrophysics*, 2<sup>nd</sup> edn. CUP, Cambridge
- Miley G., 1980, *ARA&A*, 18, 165
- Pacholczyk A. G., 1970, *Radio astrophysics*. Freeman, San Francisco
- Penrose R., 1959, *Proc. Cambridge Phil. Soc.*, 55, 137
- Rees M. J., 1966, *Nature*, 211, 468
- Rindler W., 1977, *Essential Relativity*, second edn. Springer-Verlag, New York, Heidelberg, Berlin
- Rybicki G. B., Lightman A. P., 1979, *Radiative processes in astrophysics*. Wiley-Interscience, New York
- Sikora M., Madejski G., Moderski R., Poutanen J., 1997, *ApJ*, 484, 108
- Stawarz Ł., Sikora M., Ostrowski M., 2003, *ApJ*, 597, 186
- Swift C. M., Hughes P. A., 2008, in Rector T., De Young D. S., eds, *Extragalactic jets: Theory and observation from radio to gamma-ray* Vol. 386 of *Astronomical Society of the Pacific Conference Series*, Understanding the origin of bright features. p. 429
- Tavecchio F., Maraschi L., Sambruna R. M., Urry C. M., 2000, *ApJ*, 544, L23
- Terrell J., 1959, *Physical Review*, 116, 1041
- Aloy M.-Á., Martí J.-M., Gómez J.-L., Agudo I., Müller E., Ibáñez J.-M., 2003, *ApJ*, 585, L109
- Beck R., Krause M., 2005, *Astronomische Nachrichten*, 326, 414
- Begelman M. C., Blandford R. D., Rees M. J., 1984, *Rev. Mod. Phys.*, 56, 255
- Bicknell G. V., Begelman M. C., 1996, *ApJ*, 467, 597
- Blandford R. D., Königl A., 1979, *ApJ*, 232, 34
- Burbidge G. R., 1959, *ApJ*, 129, 849+
- Celotti A., Ghisellini G., Chiaberge M., 2001, *MNRAS*, 321, L1
- Einstein A., 1905, *Annalen der Physik*, 322, 891
- Fender R. P., Belloni T. M., Gallo E., 2004, *MNRAS*, 355, 1105
- Ghisellini G., 2000, in Casciaro B., Fortunato D., Francaviglia M., Masiello A., eds, *Recent Developments in General Relativity Special Relativity at Action in the Universe*. pp 5—+
- Hardee P. E., 2003, *ApJ*, 597, 798
- Harris D. E., Krawczynski H., 2002, *ApJ*, 565, 244
- Harris D. E., Krawczynski H., 2006, *ARA&A*, 44, 463
- Harris D. E., Krawczynski H., 2007, in *Revista Mexicana de Astronomía y Astrofísica*, vol. 27 Vol. 27 of *Revista Mexicana de Astronomía y Astrofísica Conference Series*, Constraints on the Nature of Jets from KPC Scale X-Ray Data. p. 188
- Jester S., Harris D. E., Marshall H. L., Meisenheimer K., 2006, *ApJ*, 648, 900
- Königl A., Choudhuri A. R., 1985, *ApJ*, 289, 173
- Liebovitch L. S., 1974, *QJRAS*, 15, 141
- Lind K. R., Blandford R. D., 1985, *ApJ*, 295, 358
- Liu F. K., Zhang Y. H., 2002, *A&A*, 381, 757
- Longair M., 1994, *High-energy astrophysics*, 2<sup>nd</sup> edn. CUP, Cambridge
- Miley G., 1980, *ARA&A*, 18, 165
- Pacholczyk A. G., 1970, *Radio astrophysics*. Freeman, San Francisco
- Penrose R., 1959, *Proc. Cambridge Phil. Soc.*, 55, 137
- Rees M. J., 1966, *Nature*, 211, 468
- Rindler W., 1977, *Essential Relativity*, second edn. Springer-Verlag, New York, Heidelberg, Berlin
- Rybicki G. B., Lightman A. P., 1979, *Radiative processes in astrophysics*. Wiley-Interscience, New York
- Sikora M., Madejski G., Moderski R., Poutanen J., 1997, *ApJ*, 484, 108
- Stawarz Ł., Sikora M., Ostrowski M., 2003, *ApJ*, 597, 186
- Swift C. M., Hughes P. A., 2008, in Rector T., De Young D. S., eds, *Extragalactic jets: Theory and observation from radio to gamma-ray* Vol. 386 of *Astronomical Society of the Pacific Conference Series*, Understanding the origin of bright features. p. 429
- Tavecchio F., Maraschi L., Sambruna R. M., Urry C. M., 2000, *ApJ*, 544, L23
- Terrell J., 1959, *Physical Review*, 116, 1041